Third International Conference on Construction in the 21st Century (CITC-III)
"Advancing Engineering, Management and Technology"
15-17, September 2005, Athens

Seismic Behaviour of Reinforced Concrete Columns With Rectangular Spiral Shear Reinforcement

Chris G. Karayannis
Professor, Department of Civil Engeneering
Democritus University of Thrace, Xanthi, Greece, GR

George M. Sirkelis
Civil Engineer, MSc, Doctoral Candidate, Department of Civil Engeneering
Democritus University of Thrace, Xanthi, Greece, GR

Abstract
In this study the innovative technology of applying continuous rectangular spiral reinforcement as shear reinforcement of reinforced concrete columns (instead of stirrups) under seismic loading is experimentally investigated. The experimental program comprises two exterior beam–column joints. The length of the column part is equal to 1.80 m and the cross section is 20×20 cm. The beam length is 1.10 m and the cross section 20/30 cm. The first of the specimens has continuous rectangular spiral shear reinforcement whereas the latter has common stirrups. Both specimens have been suffered the same full cyclic loading with increasing deformation, 2 full cycles at every step. From the results we can see that the specimen with rectangular spiral reinforcement has shown a better response in terms of maximum loads and hysteretic energy absorption compared to the one of the specimen with the stirrups.

Keywords
Columns, Rectangular Spiral, Shear Reinforcement

1. Introduction

It is generally accepted that the use of continuous spiral reinforcement in reinforced concrete elements with cyclic cross section can substantially improve the strength and the ductility of the concrete and henceforth the total seismic response and capacity of the structural element (Park & Paulay 1975, Saatcioglu & Razvi 1992, Sheikh & Toklucu 1993). International codes in these cases propose increased performance factors for the concrete confinement (ACI 318, EC8).

The extension of the use of continuous spiral reinforcement in elements with rectangular cross sections is a new promising technology that is believed it can improve the seismic capacity of structures.

It is generally acceptable that the beam-column joints and especially the external joints are critical regions for the total seismic response of reinforced concrete structures. Moreover, the behaviour of columns is also critical for the overall seismic capacity of structures. Thus, any improvement of the seismic properties of these members using the Rectangular Spiral Reinforcement (RSR) would be very interesting in terms of general reinforcing strategy and structural safety.

The response of beam – column joints depends on some special factors as the mechanisms of shear transfer, the concrete compressive and shear strengths, the confinement of the joint area, the anchorage type of the

beam's longitudinal reinforcement etc (Paulay & Priestley 1992, Karayannis et al 1998, Karayannis & Sirkelis 2002, 2003, Tsonos 1995, 2003). It is obvious that the improvement of the concrete response in terms of any of these factors would help to the improvement of the total seismic response of the joint. Considering that the application of the RSR could contribute to the improvement of the concrete properties it is expected to contribute to the total improvement of the response of the joints.

The scope of this study is the experimental investigation of the potential improvement of seismic capacity of concrete members using continuous rectangular spiral shear reinforcement in the column and the joint body.

The results from the specimen reinforced with spiral reinforcement are compared with the results from specimen reinforced with stirrups, in terms of hysteretic response, ductility and energy absorption.

2. Experimental Program

The experimental program comprises two specimens of concrete beam – column joints. The characteristics of both specimens are presented in Table 1.

The geometric characteristics of the specimens (Table 1) were the same for both specimens. The total column length was 180 cm and the column cross-section was 20×20 cm. The column's reinforcement was 4∅10. The column's shear reinforcement was ∅8/15. The total beam length was 110 cm and the beam cross-section was 20/30 cm. The beam reinforcement was 4∅10 (2∅10 up, 2∅10 down). The beam's shear reinforcement was ∅8/15. The beam's reinforcement anchorage of specimens has the recommended by the code total length, but the anchorage had smaller straight part than the recommended one.

Specimens AJ1s and AJ1sp had 1 stirrup and one spiral step of Rectangular Spiral Reinforcement (RSR), respectively, as shear reinforcement in the joint area.

The concrete mean compressive strength for both specimens of Group A was f_c=32.8 MPa. Column axial load N_c equal to 70 kN was applied during the test in both specimens.

Table 1: Specimen characteristics

1.

Beam – Column Spesimens	
Column cross section: 20x20 cm Longitudinal bars : 4∅10 Shear reinforcement : ∅8/15	**Beam** cross section: 20/30 cm Longitudinal bars: 2∅10 Up, 2∅10 Down Shear reinforcement : ∅8/15
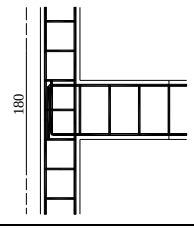	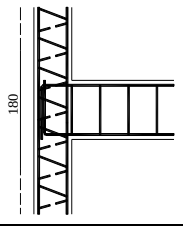
Specimen AJ1s: 1 stirrup ∅8/15 in the joint body	**Specimen AJ1sp:** 1 spiral step ∅8/15 in the joint body

2.

3.

4. 2.1 Test ring and loading procedure

5.

Test setup and instrumentation details for the experimental program are shown in Figure 1. Supports that allow rotation were used to simulate the inflection points assumed to occur at the mid-height of the columns in a laterally - loaded frame structure. Column axial load N_c=70 kN (≈0.05$A_c f_c$), was applied during the tests in both specimens.

3. 4. 2

5.

The specimens were subjected to full cyclic deformations with increasing amplitude imposed near the free end of the beam (Figure 1a) by a pinned-end actuator. Both specimens have been suffered the same increasing deformation with 2 full cycles at every step. Maximum displacements of beam's free end in the loading cycles were ±6mm, ±20mm, ±40mm and ±60mm for the 1st, 2nd, 3rd, and 4th loading step, respectively (Figure 1b). The displacements of the beam's end were measured by a LVDT (Linear Variable Differential Transformer). LVDTs were also placed at each end of the column to check the supports during the tests.

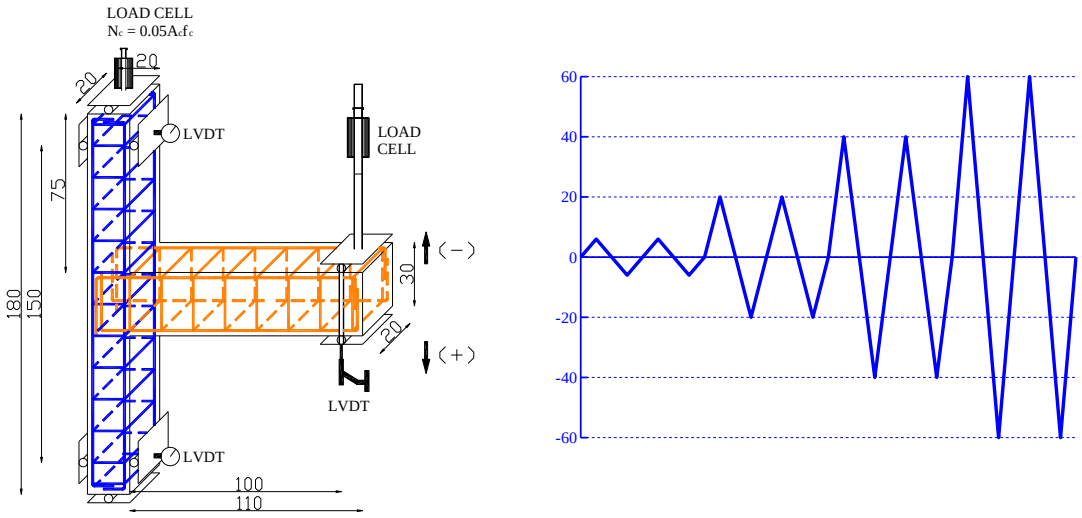

a) Test set up **b) Loading History**

Figure 1: Test set up and loading history

3 Failure Mechanisms

3.1 Joint shear strength

The failure mechanism of the specimens depends mainly on the shear strength of the joint body based on the diagonal strut mechanism.

The geometry and the forces acting on a typical external beam-column joint as free body under seismic loading are presented in Figure 2. The horizontal shear force V_{jh} acting in the joint body is equal to

$$V_{jh} = T_1 - V_{col} \quad (1)$$

where T_1 is the yield force of the longitudinal bars of the beam.

And $V_{jh} = D\cos\theta$ (Figure 3).

where D is the compression force acting in the diagonal strut and $\theta = \tan^{-1}\left(\frac{h'_b}{h''_c}\right)$

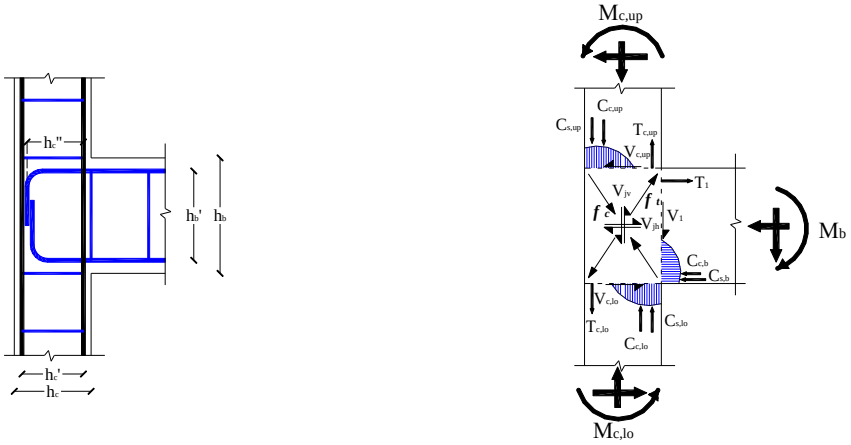

26. Figure 2: Geometry and forces acting in external beam-column joint under seismic loading

27.

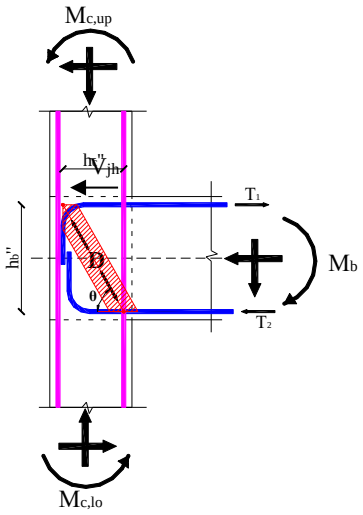

28.

29. Figure 3: Diagonal strut mechanism

30.

31.

32. The active concrete core of the joint A_{str} is equal to

33.

34. $$A_{str} = \alpha_s \times b_s \quad (2)$$

35.

where $\alpha_s = \alpha_c = \left(0.25 + 0.85\frac{N}{A_g f_c}\right) h_c''$ and b_s the width between the beam's longitudinal bars.

36.

37. It has been observed that the cracked reinforced concrete under compression loading exhibits lower strength and stiffness than uniaxially compressed concrete (compression softening phenomenon) and decreases the shear strength of the beam-column joint.

38.

39. The average principal stress of the concrete σ_d in the direction of the diagonal strut is taken equal to

40.

41. $$\sigma_d = \zeta f_c' \left[2\left(\frac{\varepsilon_d}{\zeta\varepsilon_0}\right) - \left(\frac{\varepsilon_d}{\zeta\varepsilon_0}\right)^2 \right] \text{ for } \frac{\varepsilon_d}{\zeta\varepsilon_0} \le 1 \quad \text{(Zhang \& Hsu)} \quad (3)$$

3. 4. 4

5.

42. where the softening coefficient ζ is equal to
43.
44. $$\zeta = \frac{5.8}{\sqrt{f_c'}} \frac{1}{\sqrt{1+400\varepsilon_r}} \le \frac{0.9}{\sqrt{1+400\varepsilon_r}} \quad \text{(Zhang \& Hsu)} \qquad (4)$$
45.

where $f_{c'}$ the compressive concrete strength in MPa
ε_d και ε_r the average principal strains

and $\varepsilon_r = \varepsilon_h + (\varepsilon_h - \varepsilon_d)\cot^2\theta$

and ε_o the concrete cylinder strain corresponding to the cylinder strength $f_{c'}$ and is equal to

$$\varepsilon_o = -0.002 - 0.001\left(\frac{f_c' - 20}{80}\right) \qquad \text{for } 20 \le f_{c'} \le 100 \text{ MPa}$$

Based on the equation (3) it is deduced that the joint shear strength is reached when the stress and strain of the concrete diagonal strut conform to the following equations:

$\sigma_d = \zeta f_{c'}$
$\varepsilon_d = \zeta \varepsilon_o$
46.
47. Thus the maximum compression stress $\sigma_{d,max}$ developed in the diagonal strut is equal to $\sigma_{d,max} = \zeta \times f_c, = D/A_{str}$.
48.
49. When $D < \sigma_{d,max} \times A_{str,}$ yield failure of the longitudinal bars of the beam is expected before the compressive failure of the diagonal strut
50.
51. For the examined specimens it holds that:
52.
53. $T_1 = 91.68$ kN, $V_{col} = 17.64$ kN, $\theta = 58.39^o$, $A_{str} = 7561$ mm^2, $\zeta = 0.80$
54.
55. So the maximum diagonal compressive force that could be developed in the diagonal strut (corresponding to the yield force of the longitudinal beam bars) is equal to D = 141.28 kN
56.
57. Consequently the maximum stress that can be developed in the diagonal strut is equal to $\sigma_{d,max} = 26{,}24$ MPa
58.
59. $D = 141.28 \text{ kN} < \sigma_{d,max} \times A_{str} = 198.44$ kN
60.
61. Thus it is deduced that no damages are expected in the joint body.
62.
63. 3.2 The influence of the straight part of the beam's bar anchorage
64.
65. The failure mechanism also depends on the length of the straight part of the longitudinal reinforcement anchorage.
66.
67. It is considered that the bond stress, τ, is uniformly distributed in the straight part of the beam's bar anchorage, as shown in Figure 4.
68.

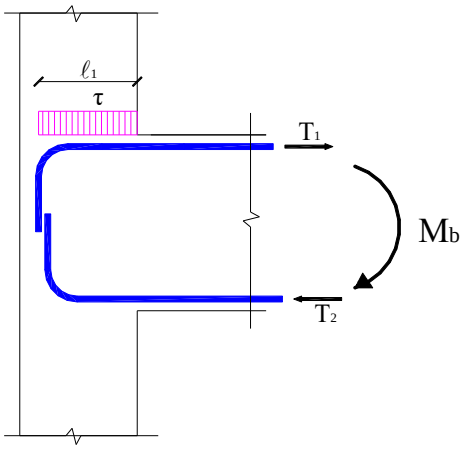

69.

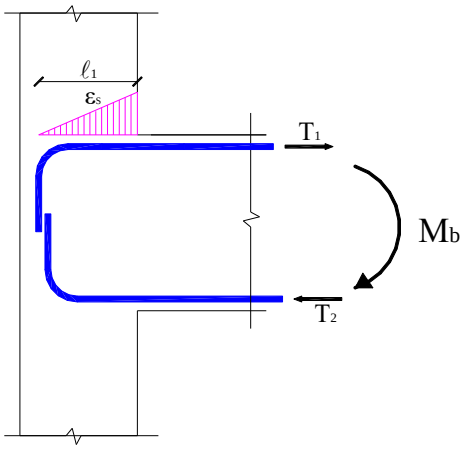

70.

71. **Figure 4: Uniformly distribution of bond stress**

72.

73. The bond stress that is developed in the reinforcement is equal to

74.

75. $$\tau = \frac{f_s A_s}{\ell_1 \pi \varnothing} \qquad (5)$$

76.

77. From the stress distribution it can be deduced that the slip s at every point of the straight part of the anchorage is equal to

78.

79. $$s = \int_0^{\ell_1} \varepsilon_s d(x) = \frac{2\tau \ell_1^2}{E\varnothing} \qquad (6)$$

80.

where $\varepsilon_s(x) = \frac{4\tau}{E\varnothing} x$

81. The CEB-FIB Model Code 90 proposes the local bond stress-slip model presented on Figure 5.

82.

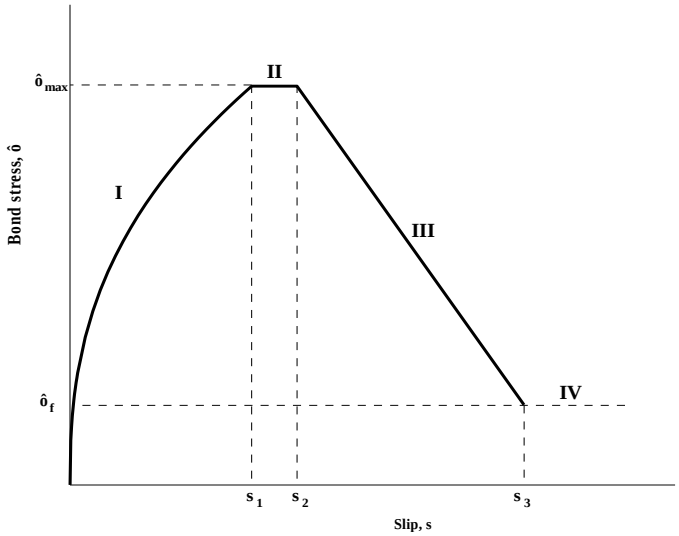

83.

84. Figure 5: Analytical bond stress – slip relationship

85.

86. where

87.

3. 4. 6

5.

88. Curve Is1 : $\tau = \tau_{max}\left(\frac{s}{s_1}\right)^a$ for $0 \le s \le$ (7)

89.
90.
91. For unconfined concrete with good bond conditions the factors in equations (7) are equal to : s_1 = 0.6 mm, α = 0.4, $\tau_{max} = 2.0\sqrt{f_{ck}}$

92. For concrete with good confinement and good bond conditions the factors above are equal to: s_1 = 1.0 mm, α = 0.4, $\tau_{max} = 2.5\sqrt{f_{ck}}$

93.

94. The maximum bond stress τ_{max} that can be developed based on the conditions of the confinement and it can take values between $2.0\sqrt{f_{ck}}$ and $2.5\sqrt{f_{ck}}$ ($2.0\sqrt{f_{ck}} \le \tau_{max} \le 2.5\sqrt{f_{ck}}$)

95.
96. The concrete confinement increases the concrete strength as follow:
97.
98. $f_c^* = f_c'\left(1 + 2{,}5\alpha\omega_w\right)$ for $\omega_w < 0.1/\alpha$

(9)

99.
100. $f_c^* = f_c'\left(1.125 + 1{,}25\alpha\omega_w\right)$ for $\omega_w > 0.1/\alpha$

(10)

101.

where ω_w : the mechanical volumetric ratio of confining hoops, equal to ω_w =(volume of confining hoops / volume of concrete core)×(f_{yd}/f_{cd})

α : confinement effectiveness factor, equal to $\alpha=\alpha_n\times\alpha_s$, with:

$$\alpha_n = 1 - \frac{8}{3n}$$

and i) for rectangular stirrups: $\alpha_s = \left(1 - \frac{s}{2b_0}\right)^2$ (Eurocode 8 – Draft 2003) (11)

ii) for rectangular spiral reinforcement : $\alpha_s = \left(1 - \frac{s}{2b_0}\right)$ (Eurocode 8 – Draft 2003) (12)

where s : the distance between the shear reinforcement

b_o : the length of shear reinforcement

For the specimens of experimental program the above factors are equal to:

Specimen	ω_w	α_n	α_s	α	f_c^*
AJ1s	1.536	0.33	0.31	0.1	43.46
AJ1sp	1.536	0.33	0.56	0.19	48.43

If k confinement coefficient ($k = \frac{f_c^*}{f_c'}$) and $k' = \sqrt{k}$

the maximum bond stress that could be developed is equal to $\tau_{max} = 2k' \sqrt{f_{ck}}$

For specimen AJ1s, $k' = 1{,}15 \Rightarrow \tau_{max} = 2.3\sqrt{f_{ck}} = 11.45$ MPa

For specimen AJ1sp, $k' = 1{,}22 \Rightarrow \tau_{max} = 2.44\sqrt{f_{ck}} = 12.15$ MPa

102.

103. In Figure 6 the bond stress – slip relationship for specimens AJ1s and AJ1sp is presented.

104.

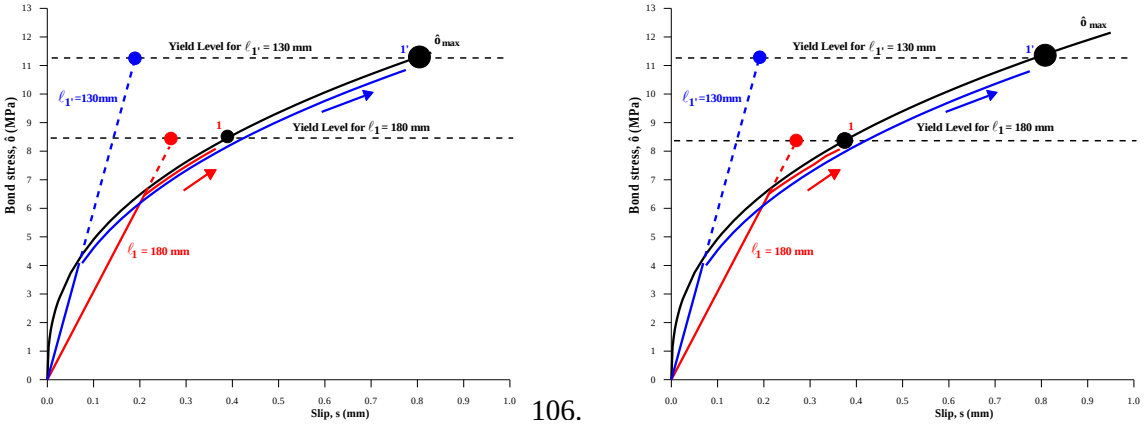

105. 106.

107. a) Specimen AJ1s **b) Specimen AJ1sp**

108. Figure 6: Bond stress – slip relationship for specimen AJ1s and AJ1sp

109.

110.

111. In Figure 6 it is shown that the straight part ℓ_1 = 180 mm of the anchorage is not sufficient and a slip of the reinforcement is occurred till the yield of the reinforcement. When yield failure of longitudinal beam's bar occurred a plastic hinge is formatted. After the yield the straight part of the anchorage is reduced due to the yield penetration of the steel bar in the joint body. Considering this penetration equal to 5∅ the available straight part of the anchorage becomes equal to $\ell_{1'}$ = 130 mm. In specimen AJ1s the yield level of $\ell_{1'}$ is very close to the maximum bond stress τ_{max} (Figure 6a) and pull out of the anchorage occurred and a crack in the joint area is observed. At the same time the back side of the joint area is cracked because of the internal push of the beam's reinforcement vertical part of anchorage (Figure 7).

112.

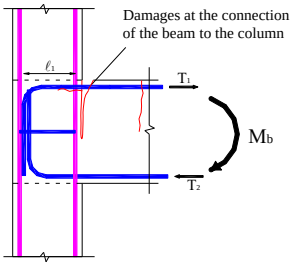

113. 114. (a)

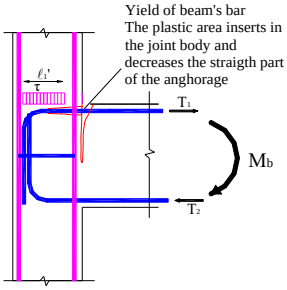

115. 116. (b)

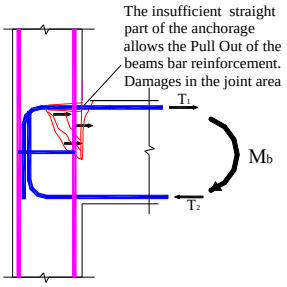

117.

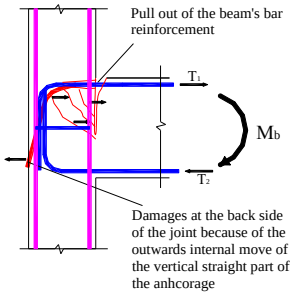

119.

118. (c)

120. (d)

121. **Figure 7: Failure mechanism of specimen AJ1s.**

122.

123. In specimen AJ1sp the yield level of $\ell_{1'}$ does not reach the maximum bond stress τ_{max} (Figure 6b) and no pull out of the anchorage is occurred. The application of the spiral reinforcement which has two points that can restrain the outward movement of the vertical part of the anchorage did not allow in the examined specimen the formation of the crack at the back side of the joint area (Figure 8).

124.

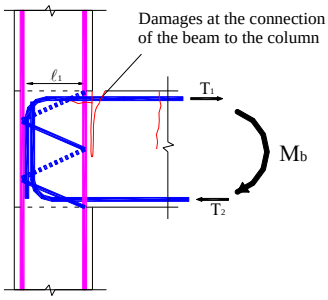

125.

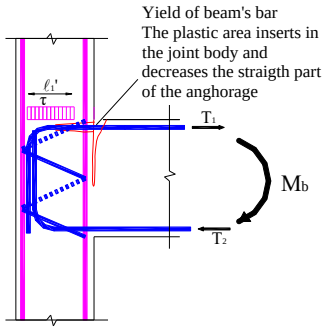

127.

126. (a)

128. (b)

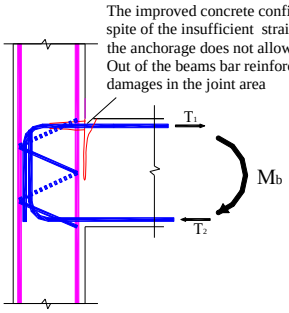

129.

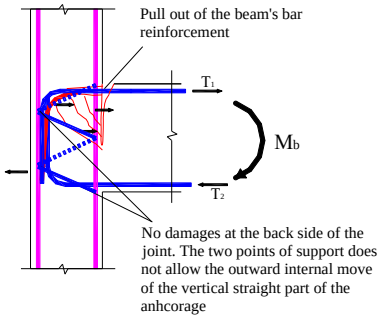

131.

130. (c)

132. (d)

133. **Figure 8: Failure mechanism of specimen AJ1sp.**

134.

135.

136. 4 Experimental results

137.

Specimens AJ1s and AJ1sp had one stirrup and one spiral step of RSR as shear reinforcement in the joint body, respectively. Both were suffered a full cyclic increasing deformation with maximum displacements of loading steps equal to ±6, ±20, ±40 and ±60 mm.

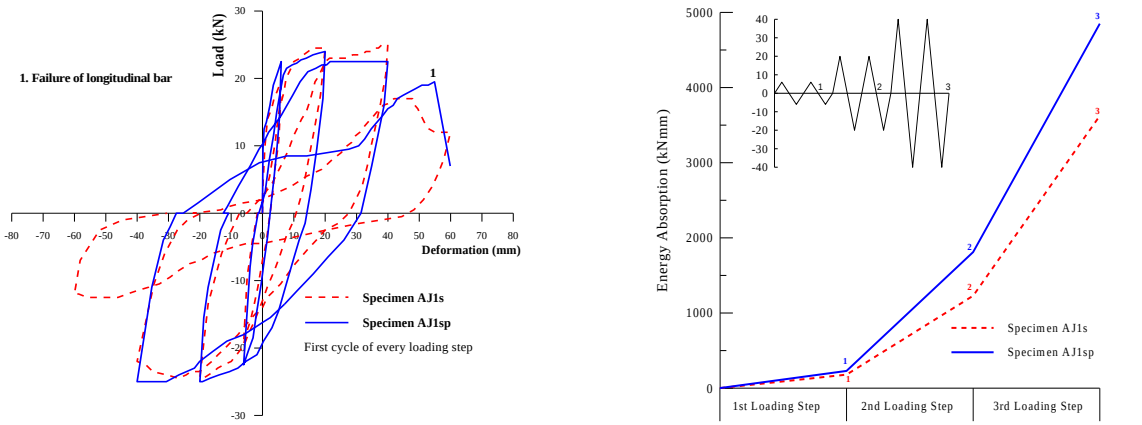

Figure 9: Hysteretic response and Energy absorption of specimens AJ1s and AJ1sp.

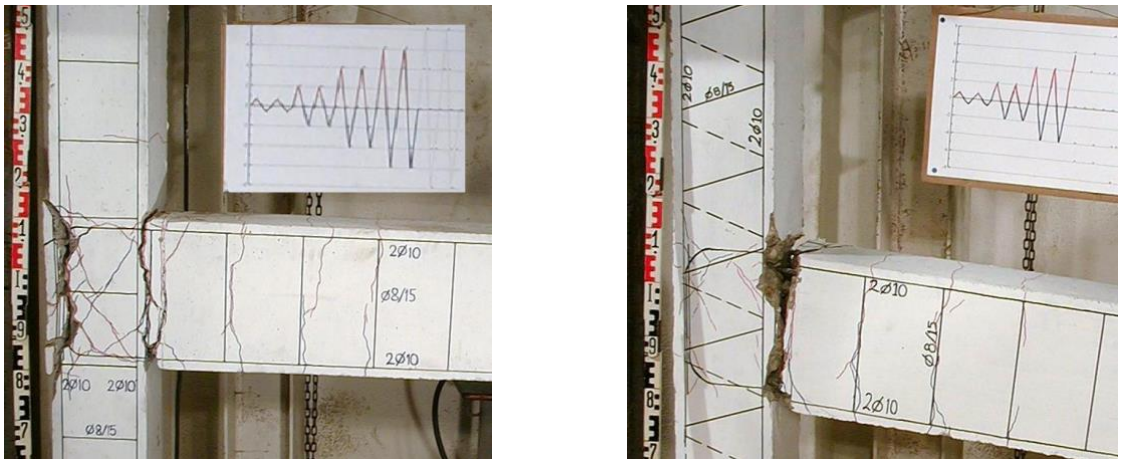

Figure 10: Final condition of specimens AJ1s and AJ1sp.

In specimen AJ1s the damage occurred at the joint area (Figure 10). The specimen kept its load carrying capacity until the fourth loading step at deformation equal to 60mm. At this deformation the back side of the joint area was cracked because of the internal push of the beam's reinforcement anchorage.

The behaviour of specimen AJ1sp was different than the behaviour of specimen AJ1s. The damage was localized from the beginning at the juncture of the beam to the column. There were no damages at the joint body (Figure 10). The specimen appeared a better behaviour in terms of energy absorption (Figure 9). Finally the damage remained only at the beam's critical region where the formation of a clear plastic hinge took place. When the deformation was equal to 60mm a failure of one longitudinal beam bar reinforcement occurred. Until the end of the loading procedure the joint body remained almost intact. This behaviour is considered as a desirable one since the damage appeared and remained outside of the joint body and had flexural characteristics. The hysteretic response of specimen AJ1sp was improved compared to the one of the specimen AJ1s by 34% in terms of energy absorption.

138.

139. 5. Conclusions

140.

In this study results from specimen of concrete columns, tested in cyclic loading, reinforced with Rectangular Spiral Reinforcement (RSR) are compared with the results of similar specimen reinforced with typical stirrups equally spaced and tested the same way.

3. 4. 10

5.

In specimen reinforced with stirrups (AJ1s) the damage was appeared and localized at the joint body. On the contrary in the specimen reinforced with RSR (AJ1sp) the damage appeared only at the beam's critical region with the formation of a plastic hinge. This behaviour is considered as the best expected one since the damages remained outside of the joint body and appeared mainly flexural (ductile) characteristics. Finally, the hysteretic response of specimen AJ1sp was improved compared to the one of the specimen AJ1s by 34% in terms of energy absorption.

6. References

141.

Essawy A.S.; El-Havary M. (1998) "Strength and ductility of spirally reinforced rectangular concrete columns". *Journal Construction and Building Materials,* Vol. 12. No 1, pp. 31-37.

Karayannis C.G.; Chalioris C.E.; Sideris K.K. (1998). "Effectiveness of RC Beam-Column Connection Repair Using Epoxy Resin Injections". *Journal of Earthquake Engineering,* Vol.2. No 2, pp. 217-240.

Karayannis C.G.; Sirkelis G.S. (2002). "Effectiveness of RC Beam-Column Connections Strengthening Using Carbon-FRP Jackets". *12th ECEE*. Proc. in CD form, paper ref. 549.

Karayannis C.G.; Sirkelis G.S.; Chalioris C.E.; Mavroidis P. (2003). "External R.C. Joints with continuous spiral reinforcement. Experimental investigation". *14th Greek Concrete Conference*, Vol. A, pp. 343-353, In Greek.

Karayannis C.G.; Sirkelis G.S. (2003). "Design parameters and response of external joints-Damage index and valuation of experimental results". *14th Greek Concrete Conference*, Vol. A, pp. 332-342, In Greek.

Karayannis C.G.; Sirkelis G.S. (2003). "Effectiveness of RC Beam-Column Connections Strengthening Using Carbon-FRP Jackets". *12th European Conference on Earthquake Engineering (12ECEE),* Paper Ref.549.

Park R.; Paulay T. (1975) "*Reinforced Concrete Structures*". John Wiley & Sons.

Paulay T.; Priestley M.J.N. (1992). "*Seismic design of reinforced concrete and masonry buildings*". John Wiley & Sons.

Saatcioglu M.; Razvi S. (1992). "Strength and ductility of confined concrete". *Journal of Structural Engineering ASCE,* Vol. 118, No 25, pp. 1590-1607.

Sheik S.; Toclucu M.; (1993). "Reinforced concrete columns confined by circular spirals and hoops". *ACI Structural Journal,* Vol. 90, No 5, pp. 542-553.

Shyh-Jian Hwang.; Hung-Jen Lee. (1999). "Analytical model for predicting shear strengths of exterior reinforced concrete beam-column joints for seismic resistance". *ACI Structural Journal,* Vol. 96, No. 5, pp.846-857

Tsonos A. (1995). "Shear strength and hysteretic behaviour of exterior beam column connections". *Proceedings of the 5th SECED Conference on European Seismic Design Practice - Research and Application*, London, Proc. Balkema, pp.553-559.

Tsonos A.; Papanikolaou K. (2003). "Post-earthquake repair and strengthening of reinforced concrete beam-column connections (theoretical and experimental investigation)". *Bulletin of the New Zealand Society for Earthquake Engineering*, Vol. 36, pp.73-93.

Zhang L.X.B.; Hsu T.T.C. (1998). "Behavior and analysis of 100 MPa Concrete Membrane Elements". *Journal of Structural Engineering, ASCE*, Vol. 124, No1, pp. 24-34